ARKIV FÖR FYSIK Band 15 nr 33

Communicated 11 March 1959 by Erik Hulthén and Kai Siegbahn

Nuclear magnetic dipole and electric quadrupole moments of radioactive bismuth isotopes

By I. Lindgren and C. M. Johansson

With 16 figures in the text

ABSTRACT

The hyperfine structure of the neutron-deficient bismuth isotopes $Bi^{203-206}$ has been studied by the atomic beam magnetic resonance method by use of six-pole focusing and radioactive detection. The results are summarized in the following table:

Isotope	Half-life	Spin	a Mc/s	b Mc/s	μ_I n.m.	Q 10^{-24} cm²
Bi^{203}	12 hr	9/2	-502.4 ± 3.0	-558 ± 25	$+4.59 \pm 0.05$	-0.64 ± 0.05
Bi^{204}	13 hr	6	-349.0 ± 2.0	-358 ± 20	$+4.25 \pm 0.05$	-0.41 ± 0.05
Bi^{205}	14.5 d	9/2	(-600)		$(+5.5)$	
Bi^{206}	6.3 d	6	-374.7 ± 3.0	-166 ± 30	$+4.56 \pm 0.05$	-0.19 ± 0.05

The magnetic dipole moments (μ_I) are calculated from the magnetic dipole interaction constants (a) by means of the known values of a and μ_I of Bi^{209} and the Fermi-Segré formula, neglecting the hfs anomaly. In order to obtain the electrical quadrupole moments (Q) from the electric quadrupole interaction constants (b), the intermediate state of bismuth has been determined from the optically measured energy levels and from the known g_J-value of the ground state. The average of the inverse cube of the distance of the electrons from the nucleus, $\langle r^{-3} \rangle$, has been calculated from the magnetic dipole interaction in Bi^{209} and is compared with the value obtained from the spin-orbit coupling. The quadrupole moments are not corrected for the effect of distortion of the inner electron shells (Sternheimer's correction). The results are compared with theoretical values obtained from the nuclear shell model.

I. Introduction

In recent years nuclear spectroscopists have shown great interest in the isotopes of the "nuclear lead region". In this region, in the vicinity of stable Pb^{208}, the numbers of protons and neutrons are near the "magic numbers" 82 and 126, respectively, and the nuclei thus consist of closed shells with a small number of additional particles or holes. Therefore, theoretical calculations based on the simple single-particle model can be expected to be fruitful. In many cases very good agreement with experimental data has been obtained with this model.

The lead region is now an object of systematic studies by various groups in Sweden.[1] As a part of this general program the ground-state spins and moments of some neutron-deficient bismuth isotopes have been measured with the atomic beam technique. The spin values are particularly important to nuclear spectroscopists, since they often serve as a starting point in the determinations of decay schemes. In many cases it is impossible to construct a definite decay scheme or energy level diagram without knowledge of the ground-state spin. The moments are also interesting from a theoretical point of view. Together with the spin values they can be used to test different nuclear models. In the lead region, in particular, more definite statements about the nuclear configurations can be made with knowledge of the magnetic moments, while the quadrupole moments can give information about the collective motions in the nuclei.

The nuclear spins of the bismuth isotopes with masses 203–206 have been reported previously [1], and these measurements have now been extended to hyperfine structure (hfs) separations, magnetic dipole moments, and electric quadrupole moments. The results are discussed in connection with calculations based on the single-particle model. For the magnetic moments the agreement between the experimental values and those obtained from the modified single-particle model is good. For the electric quadrupole moments the single-particle model gives values of the right order of magnitude, and the agreement is better nearer the closed shells.

II. The method

In these experiments we have used the focusing atomic beam resonance method, introduced by Hamilton, Lemonick, and Pipkin [2]. Since the apparatus has been described in detail in an earlier article [3], only a summary of the principles will be given here.

Figure 1 shows schematically the beam trajectories in the apparatus. In the A-magnet those atoms which have an effective magnetic moment $\mu_{\text{eff}} < 0$ are focused towards the axis, while those for which $\mu_{\text{eff}} > 0$ are defocused. With the obstacles arranged according to figure 1 only the former atoms can enter the B-magnet. This is the same type as the A-magnet, so those atoms which were focused there will also be focused in the B-magnet. Therefore, no atoms will reach the detector, unless they change their magnetic states on the way through the apparatus. In the homogeneous C-field between the A- and B-fields a radio-frequency field of the proper frequency can induce a transition in the state of the passing atom. If the transition causes μ_{eff} to change sign, the atoms which were focused in the A-magnet will be defocused in the B-magnet and can reach the detector. Since the intensity there has a maximum at resonance, this is a "flop-in" arrangement [4].

For atoms with $J = 3/2$, like those of bismuth, two flop-in transitions for which $\Delta F = 0$ may be observed, namely where $F = I + J$ and $F = I + J - 1$, $m = \mp (F - J - 1/2) \leftrightarrow m = \mp (F - J + 1/2)$. Figure 2 shows the energy as a function of the magnetic field for an atom with $J = 3/2$ and $I = 9/2$. Only the four levels involved in our experiments have been plotted completely. Once the spin has been determined at a very low field, the field strength is increased stepwise, and each new resonance

---

[1] For detailed references see the review article by I. Bergström and G. Andersson (Ark. f. Fysik *12*, 415 (1957)).

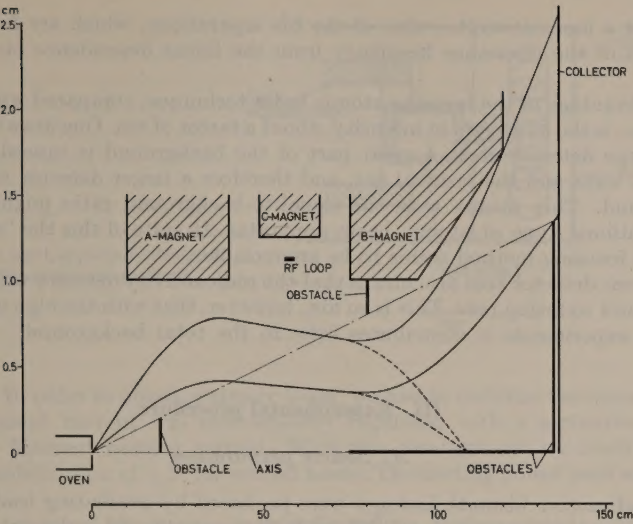

Fig. 1. A schematic view of typical beam trajectories in a six-pole focusing atomic beam apparatus. Notice the exaggerated vertical scale.

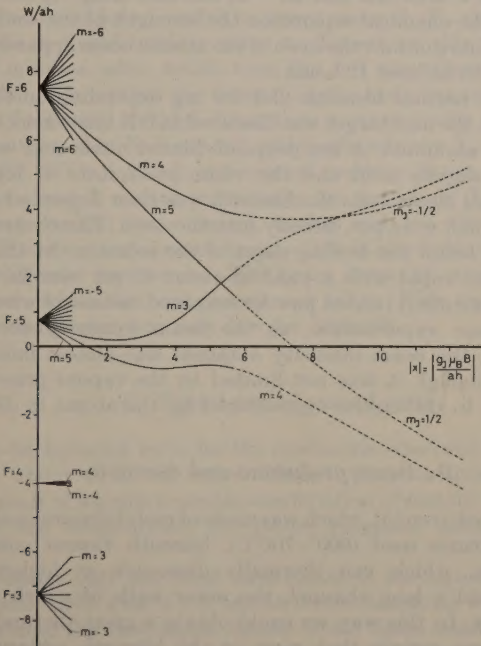

Fig. 2. The variation in a magnetic field of the energy levels of Bi^{203} ($J = 3/2$, $I = 9/2$). Only those levels which are directly involved in the experiments are drawn completely.

line gives a more accurate value of the hfs separations, which are functions of the deviation of the resonance frequency from the linear dependence on the magnetic field.

The advantage of the focusing atomic beam technique, compared with the conventional one, is the large gain in intensity, about a factor of ten. One drawback, however, is the large detector area. A great part of the background is caused by scattering from the walls and the residual gas, and therefore a larger detector causes a higher background. This means that the signal-to-background ratio might be better in a conventional type of atomic beam apparatus. In spite of this the "effective gain" with the focusing method seems to be appreciable.

The great detector area also means that the radioactivity detector will have a higher background counting rate. This is so low, however, that with the high intensities used in these experiments it contributes little to the total background.

III. Experimental procedure

A. Source preparation

The radioactive bismuth isotopes were produced by irradiating lead with protons or deutrons of various energies. Bi^{203} and Bi^{204} were produced in the synchro-cyclotron at Uppsala with 60 MeV and 30 MeV protons, respectively, Bi^{205} in the cyclotron in Stockholm with 25 MeV deutrons and Bi^{206} in the Oak Ridge cyclotron also with 25 MeV deutrons. After the chemical separation the strength of the sources was usually about 5 millicuries. When put into the oven of the atomic beam apparatus such samples gave an intense beam for at least 12 hours.

Together with some natural bismuth (0.3–3.0 mg depending on the strength and half-life of the sample), the lead target was dissolved in 6 N nitric acid, and the solution was neutralized with ammonia. A few drops of diluted nitric acid were added, until the solution became slightly acid and the white precipitate of bismuthyl nitrate redissolved. By internal electrolysis the bismuth was then deposited on nickel wires, wound into spirals, which were put directly into the oven. The electrolysis was made at a temperature just below the boiling point of the solution. At the proper acidity the procedure was very rapid with a yield of about 80 per cent in 20 minutes.

In our earlier experiments [1] nickel powder was used instead of wires. This method, however, gave a poor vaporization, as the beam intensity decreased without stabilization. Further, the beam intensity obtained was almost independent of the oven temperature, although it was not limited by the vapour pressure. These phenomena may be due to difficulties encountered by the atoms in diffusing through the nickel powder.

B. Beam production and detection

The specially designed oven [5], which was made of molybdenum, is shown in figure 3. At the oven temperatures used (600°–700°C), bismuth vapour consists mainly of polyatomic molecules, which can thermally dissociate at higher temperatures. Therefore the oven had a long channel, the outer walls of which were heated by electron bombardment. In this way we could obtain a great thermal gradient along the oven, and we were certain that most of the bismuth molecules dissociated. The temperature at the oven front was 1300°–1500°C at ordinary vaporization

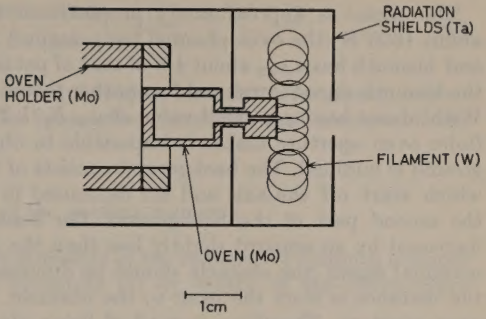

Fig. 3. The oven used, especially designed to give a high temperature gradient.

temperatures. In order to obtain a steady beam, we had to stabilize the oven heating. The bombardment current was electronically regulated with a servoarrangement acting on the filament heating current. With this arrangement we could reach a temperature stabilization of ±2° for several hours. The heating power used amounted about 150 W.

For beam detection the atoms were collected on carbon-coated copper foils. Various clean metal foils were also tried as collectors, but they all had lower sticking coefficients, even though they were cooled with liquid air. A sulfur-coated surface, which has been found useful in many cases [6, 7], also had a high sticking factor, but we have found carbon easier to deposit on thin foils. Exposures were taken for 5–10 minutes, after which time the foil was taken out of the apparatus through a vacuum lock, so that the vacuum in the main chamber was not destroyed. The radioactivity collected on the foil was then measured with a scintillation detector equipped with a very thin NaI crystal, which absorbs the X-rays following electron capture decay [6]. With a 25 × 2 mm crystal inside a 10 cm thick lead castle, the background was about 3 counts per minute for the whole X-ray line. To increase counting accuracy, we had two counters, so that each foil was counted for twice the exposure time. To detect a resonance line the C-field was held constant and exposures were made at different frequencies. The beam intensity was checked every three or four exposures, while the background was taken. This was necessary, since the signal-to-background ratio was very low for bismuth.

C. Signal-to-background ratio

The signal-to-background ratio for the resonances observed was usually about 1:2 compared with about 40:1, the value obtained for potassium. The poor value for bismuth is the result of an unfavourable combination of factors, such as the number of magnetic levels, the temperature, the atomic magnetic moment, and the isotopic dilution.

For each resonance only one level contributes to the signal, while all levels give rise to background. Bi^{204} with $I = 6$ has 52 levels compared with 8 for K^{39}. Thus for a certain background the Bi^{204} signal should be 6.5 times smaller than that from K^{39} because of the number of levels. If other activities are present in the beam, the backgrounds add and the signal-to-background ratio becomes lower.

The signal is approximately proportional to $\mu_{\text{eff}} B_0 / kT$ [3]. For bismuth T is about 1600°K (the oven channel temperature) compared with 500° K for potassium, and bismuth has a μ_{eff} about 4/5 of that of potassium. Because of these circumstances the bismuth signal is reduced by another factor of 4 compared with that of potassium. With atoms having a small value of $\mu_{\text{eff}} B_0 / kT$, there is an additional difficulty; the finite oven aperture makes it impossible to obtain maximal signal, when the background is minimal. The background consists of two parts, scattered atoms and atoms which start off the axis and are defocused in both deflecting magnets. To remove the second part of the background, the diameter of the first obstacle should be increased by an amount slightly less than the oven hole diameter, whereas to reach maximal signal, the obstacle should be diminished by the same amount. The longer the distance is from the oven to the obstacle, the smaller is the effect of the finite oven aperture. Therefore, instead of being placed at the entrance [3], the obstacle has been moved about 10 cm into the A-magnet, where the atoms are not yet greatly deflected, and there it has been dimensioned for the best signal-to-background ratio with $\mu_{\text{eff}} B_0 / kT$ about the same as that of bismuth. Nevertheless the signal-to-background ratio was 2–4 times smaller with the oven aperture used (0.4 mm) than it should have been with a point-sized oven aperture.

IV. Theory

A. Calculation of the interaction constants

The interaction between the atomic and nuclear magnetic moments and an external magnetic field can be expressed by the Hamiltonian:

$$H' = (g_J \mathbf{J} + g_I \mathbf{I}) \mu_B \mathbf{B},$$

where the g-values are defined $g_J = -\mu_J / J \mu_B$ and $g_I = -\mu_I / I \mu_B$, respectively. At low fields, where this interaction is weak compared with that between the electrons and the nucleus, the energy levels are easily obtained by the perturbation method. A low-frequency flop-in transition, for which $\Delta F = 0$ and $m = \mp (F - J + 1/2) \leftrightarrow m = \mp (F - J - 1/2)$, has the following linear and quadratic terms:

$$\nu' = \{g_J (F \vdots J_Z \vdots F) + g_I (F \vdots I_Z \vdots F)\} \frac{\mu_B B}{h},$$

$$\nu'' = \pm (g_J - g_I)^2 \left\{ \frac{(F \vdots J_Z \vdots F-1)^2}{\Delta \nu_F} - \frac{(F \vdots J_Z \vdots F+1)^2}{\Delta \nu_{F+1}} \right\} 2 (F - J) \left(\frac{\mu_B B}{h} \right)^2, \qquad (1)$$

where $(F \vdots J_Z \vdots F')$ is the part of the matrix element $(F m | J_Z | F' m)$ that is independent of m, and $\Delta \nu_F$ is the separation (with its sign) between the hfs levels F and $F - 1$ at zero field, in frequency units. In experiments with atoms with $J = 3/2$ two low-frequency flop-in transitions can be observed, which correspond to $F = I + J$ and $F = I + J - 1$ (see fig. 2). This gives the two hfs separations $\Delta \nu_{I+J}$ and $\Delta \nu_{I+J-1}$.

The interaction of the nuclear magnetic dipole and electric quadrupole moments with the atomic fields is expressed by

$$H^0 = h a \mathbf{I}\cdot\mathbf{J} + h b\,\frac{3(\mathbf{I}\mathbf{J})^2 + 3/2(\mathbf{I}\mathbf{J}) - I(I+1)J(J+1)}{2J(2J-1)I(2I-1)}; \tag{2}$$

a and b are the magnetic dipole and electric quadrupole interaction constants, respectively. By means of this expression the interaction constants are calculated from the two hfs separations obtained above.

B. Calculation of the nuclear moments

One can calculate the magnetic dipole moments of the radioactive bismuth isotopes from the magnetic dipole interaction constants (a) by means of the Fermi-Segré formula

$$\frac{g_I^{(1)}}{g_I^{(2)}} = \frac{a^{(1)}}{a^{(2)}} \tag{3}$$

with the known values of g_I and a of Bi^{209}, neglecting the hfs anomaly.

The electric quadrupole interaction constant (b) is related to the quadrupole moment (Q) by the well-known expression:

$$h b = -\frac{e^2}{4\pi\varepsilon_0}\,Q\left\langle\frac{3\cos^2\Theta - 1}{r^3}\right\rangle_{JJ}, \tag{4}$$

where the average is taken in the state $m_J = J$, summed over all electrons. In order to evaluate this average, one must know the electronic wave function. As known from optical measurements, the coupling between the electrons in bismuth is intermediate between the LS- and jj-extremes. The g_J-value of the ground state is 1.6433 as measured by the atomic beam method [8], while the corresponding values in LS- and jj-coupling are 2 and 4/3, respectively.

The wave function of the intermediate state can be expressed as a linear superposition of the eigenfunctions in either of the extreme couplings; the coefficients are functions of one parameter, which defines the state of intermediate coupling. This parameter can be chosen to give the best fit of the theoretical energy levels to the experimental ones or to give the correct g_J-value of the ground state.

The energy relationship and the Zeeman-effect in intermediate coupling have been treated in two papers by Inglis and Johnson [9, 10], whose method will be followed here. The g_J-value is obtained by transforming the g_J-matrix in the LS-coupling scheme to the intermediate state by the matrix that diagonalizes the energy matrix. The problem is thus reduced to finding the energy matrix.

The electronic ground-state configuration of bismuth is $6s^2\ 6p^3$, which gives rise to five possible states, in LS-coupling denoted by ${}^2D_{5/2}$, ${}^2D_{3/2}$, ${}^2P_{3/2}$, ${}^2P_{1/2}$, and ${}^4S_{3/2}$. The J-value in the ground state is 3/2 and, since this can be assumed to be a good quantum number, the intermediate state can be expressed as a linear superposition of the three states ${}^2D_{3/2}$, ${}^2P_{3/2}$, and ${}^4S_{3/2}$ (always taken in this order in the following).

In terms of the parameters of the spin-orbit coupling energy (A) and of the electrostatic energy (B), the energy matrix in the LS-coupling scheme becomes (with ${}^2D_{5/2}$ as reference)[1]

---

[1] The constant A used here is equal to $2A$ in ref. [9] and a in ref. [10]. The constant B is equal to B in ref. [9] and X in ref. [10].

$$H=\begin{pmatrix} 0 & A\frac{\sqrt{5}}{2} & 0 \\ A\frac{\sqrt{5}}{2} & 2B & A \\ 0 & A & -3B \end{pmatrix},$$

and the secular equation becomes

$$W^3+BW^2-(\tfrac{9}{4}A^2+6B^2)W-\tfrac{15}{4}A^2B=0. \tag{5}$$

The diagonalizing matrix has the elements

$$\left\{\begin{aligned} R_{k1}&=\frac{\sqrt{5}}{2}\,\frac{\varepsilon_k+3x}{\varepsilon_k}\,R_{k3},\\ R_{k2}&=(\varepsilon_k+3x)\,R_{k3},\\ R_{k3}&=\varepsilon_k\left[(\varepsilon_k^2+\tfrac{5}{4})\,(\varepsilon_k+3x)^2+\varepsilon_k^2\right]^{-1/2}, \end{aligned}\right. \tag{6}$$

in which $\varepsilon_k=W_k/A$, $x=B/A$, and W_k is a solution of the secular equation. By transforming the matrix of g_J (which is diagonal in the LS-scheme), we obtain the following expression for the g_J-value of the state k in intermediate coupling[1],

$$g_k'=\sum_l R_{kl}^2\,g_l=\frac{(\tfrac{4}{3}\varepsilon_k^2+1)\,(\varepsilon_k+3x)^2+2\,\varepsilon_k^2}{(\varepsilon_k^2+\tfrac{5}{4})\,(\varepsilon_k+3x)^2+\varepsilon_k^2}, \tag{7}$$

where g_l is the g_J-value of the state l in LS-coupling. By use of this expression and the secular equation (5), the parameter x can be determined to give the correct g_J-value of the ground state. The experimental value of bismuth, $g_J=1.6433$, corresponds to $x=0.300$.

The best fit of the theoretical energy levels to the experimental ones is obtained for $x\approx 0.295$ [11], in very good agreement with the value obtained from the g_J-value. For the following we use the value $x=0.30$ with an estimated uncertainty of about 0.02.

The wave function of the intermediate state is

$$\psi_k=R_{k1}\,{}^2D_{3/2}+R_{k2}\,{}^2P_{3/2}+R_{k3}\,{}^4S_{3/2},$$

where ${}^2D_{3/2}$ etc. represent the wave functions of the corresponding states. For the following, however, it will be more convenient to have the wave function expressed in the jj-coupling scheme. The transformation from LS- to jj-coupling can e.g. be performed by finding the diagonalizing matrix of the spin-orbit energy matrix in the LS-scheme.

The possible states with $J=3/2$ in jj-coupling are

$$\begin{aligned} \psi_1&=(\tfrac{3}{2}\,\tfrac{3}{2}\,\tfrac{3}{2})_{3/2},\\ \psi_2&=(\tfrac{3}{2}\,\tfrac{3}{2}\,\tfrac{1}{2})_{3/2},\\ \psi_3&=(\tfrac{3}{2}\,\tfrac{1}{2}\,\tfrac{1}{2})_{3/2}, \end{aligned}$$

---

[1] Note the misprints in the formulas corresponding to (6) and (7) in ref. [10].

and the intermediate wave function is

$$\psi = c_1\psi_1 + c_2\psi_2 + c_3\psi_3.$$

$x = 0.30$ gives the following c-values,

$$c_1 = -0.177,\ c_2 = 0.318,\ \text{and}\ c_3 = 0.932.$$

Schüler and Schmidt [12] have given the equation

$$\left\langle\frac{3\cos^2\Theta - 1}{r^3}\right\rangle_{JJ} = \frac{2}{5}\left[(c_1^2 - c_3^2)\,R_r' + 2\sqrt{\frac{2}{5}}\,c_2\,(c_1 + c_3)\,S_r\right]\langle r^{-3}\rangle_{cl}, \tag{8}$$

in which the subscript $_{cl}$ indicates the non-relativistic value, and R_r' and S_r are relativistic corrections, tabulated by Kopfermann [13].

The value of $\langle r^{-3}\rangle_{cl}$ can be obtained without knowledge of the explicit wave function, either from the nuclear magnetic dipole interaction or from the electron spin-orbit interaction in Bi^{209}. Breit and Wills [14] have treated the hfs in intermediate coupling, and from their calculations we obtain the following expression for the magnetic dipole interaction constant (a),

$$h\,a = -\frac{\mu_0}{4\pi}\,g_I\,\mu_B^2\left[\frac{16}{15}\left(1 + \frac{1}{5}c_2^2\right)F' - \frac{16}{15}c_2^2\,F'' + \frac{4}{3}\sqrt{\frac{2}{5}}\,c_2\,(c_1 - c_3)\,G\right]\langle r^{-3}\rangle_{cl}. \tag{9}$$

The relativistic corrections F', F'', and G are tabulated by Kopfermann [13]. The effects of distortion of inner electron shells (Sternheimer [15]) and of configuration interaction (Koster [16]) have not been considered here. With the experimental values of a and g_I of Bi^{209} ($a = -446.97$ Mc/s [8], $\mu_I = 4.0797$ n.m., and $I = 9/2$ [17]) and the c-values calculated above, this equation gives[1]

$$\langle r^{-3}\rangle_{cl} = 1.35\cdot 10^{12}\,\frac{4\pi h}{\mu_0\,\mu_B^2}.$$

The "effective" nuclear charge $Z_i = 77$ [19] has been used in the relativistic corrections.

From the spin-orbit coupling energy the following expression for $\langle r^{-3}\rangle_{cl}$ is obtained [12],

$$\langle r^{-3}\rangle_{cl} = \frac{4\pi A h}{2\,\mu_0\,H_r\,Z_i\,\mu_B^2},$$

in which A is the parameter of the spin-orbit coupling in frequency units and H_r is a relativistic correction [13]. $A = 3.03\cdot 10^8$ Mc/s [11] and $Z_i = 77$ [19] gives

$$\langle r^{-3}\rangle_{cl} = 1.68\cdot 10^{12}\,\frac{4\pi h}{\mu_0\,\mu_B^2}.$$

The discrepancy between the two values of $\langle r^{-3}\rangle_{cl}$ is probably due mainly to the uncertainties in Z_i and the state of intermediate coupling. An increase of the x-value of about 0.04 would give agreement between the two determinations. The quadrupole moments are, however, rather insensitive to small changes in the x-value. With the value of $\langle r^{-3}\rangle_{cl}$ from the hfs ($x = 0.30$), equations (4) and (8) give

---

[1] This equation gives positive sign of the dipole interaction constant in contradiction to optical measurements [18].

$$\frac{Q}{b} = -\frac{4\pi\varepsilon_0 h}{e^2\left\langle \frac{3\cos^2\Theta - 1}{r^3}\right\rangle_{JJ}} = 1.14\cdot 10^{-3}, \tag{10}$$

in which Q is expressed in 10^{-24} cm^2 and b in Mc/s. An error of 0.02 in the x-value causes a change in this ratio of only about one per cent. The Sternheimer correction of this ratio has been calculated to be 1.019 for bismuth [15], without consideration of the antishielding effect. The latter has not been calculated but may predominate over the shielding effect [15, 20]. Therefore, the uncorrected quadrupole moments are probably somewhat too large.[1]

V. Results

The resonance frequencies of the two lines of Bi^{203}, Bi^{204}, and Bi^{206} at different magnetic fields are tabulated below, and the curves at the highest fields, which are most significant, are reproduced. Since the signal-to-background ratio is rather low and the intensity usually varies during a measurement (because of radioactive decay and changes in evaporation rate), the intensity has been normalized to a constant background. In the figures this background has been subtracted. The given uncertainty is the statistical one, not including the uncertainty in intensity, which, however, can be assumed to be comparatively small.

The peak of the resonance curve can usually be determined with an accuracy of about one-tenth of the line-width. The peak need not necessarily coincide with the true resonance frequency. If, e.g., the rf-power is higher than the optimal one, the line may be shifted, probably due to the fact that the effective rf-field becomes longer. It has been found that this shift is larger for an unsymmetrical than for a symmetrical line. Regarding this, the uncertainty in the resonance frequency has been chosen to be as large as about one-fourth of the line-width if the curve is symmetrical and if the statistics are good, and somewhat more in other cases. The consistency of the results shows that the probability for a larger error is very small.

The magnetic field has been calibrated with K^{39}. The uncertainty in this case has been taken to be about one-tenth of the line-width, since the appropriate rf-power can easily be chosen. In some cases the field is also measured with the K^{41}-line, and the consistency shows that the field measurement is free from any appreciable systematic errors. The field has always been checked both before and after measuring a line and the uncertainty given also includes the drift.

The tables below give the values of the quadratic term of the frequency (ν'') divided by $(\mu_B B/h)^2$. The calculations have been made by use of fourth-order perturbation theory and have been checked by diagonalizing the energy matrices. The discrepancy between the results of the two methods corresponds in all cases to an error less than 1 kc/s in the resonance frequency. The g_J-value 1.6433 ± 0.0002, given by Smith [8], has been used.

---

[1] A small admixture of a configuration containing unpaired s-electrons could have a considerable effect on the result above [16]. To avoid this difficulty the value of $\langle r^{-3}\rangle_{cl}$ can be taken from the spin-orbit coupling. In this case, however, the uncertainty in the degree of intermediate coupling has a larger effect. The result becomes $Q/b = (0.92 \pm 0.20)\cdot 10^{-3}$, which is not in disagreement with the value obtained by means of the magnetic hfs. Again, the Sternheimer correction is omitted.

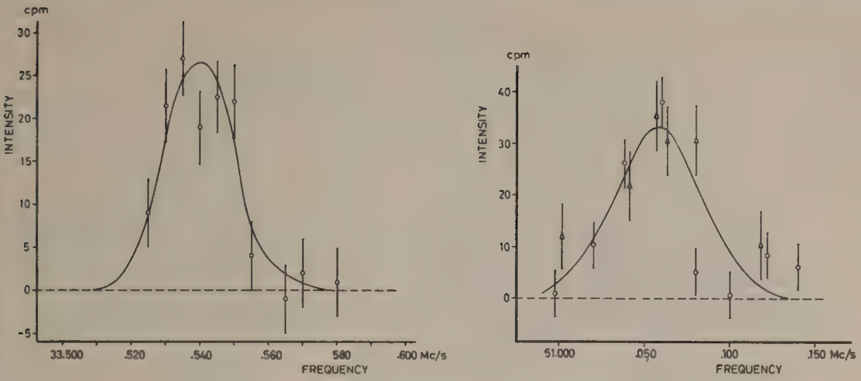

Fig. 4.

Fig. 5.

Figs. 4, 5. Resonance curves of Bi^{203}, ($F = 6$).

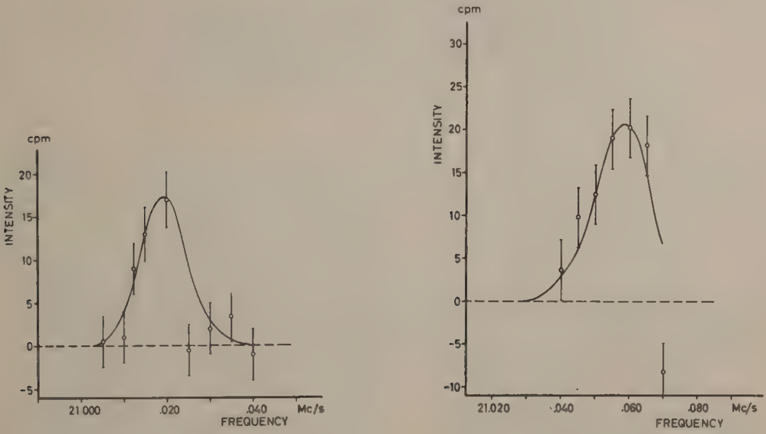

Fig. 6.

Fig. 7.

Figs. 6, 7. Resonance curves of Bi^{203}, ($F = 5$).

The value of $\nu''/(\mu_B B/h)^2$ has been calculated with the assumption of positive and negative nuclear magnetic moments, respectively. If the right sign is chosen, the values at different fields should be consistent with each other, while in the opposite case they should increase or decrease monotonically with the field. As is seen from the tables, the resolution is good enough that the signs of the moments can be determined definitely.

Table 1. Bi^{203}.

Ref.	ν_{ref}	$\frac{\mu_B B}{h}$	ν	$\nu''\Big/\left(\frac{\mu_B B}{h}\right)^2 \times 10^6$		Remarks
				$\mu_I > 0$	$\mu_I < 0$	
$F=6$						
	17.766 ± 6	31.946 ± 10	13.244 ± 10	130 ± 11	104 ± 11	Fig. 16, ref. [3]
	30.902 ± 10	51.963 ± 15	21.657 ± 5	121.7 ± 3.0	105.7 ± 3.0	
	30.897 ± 10	51.956 ± 15	21.655 ± 5	122.0 ± 3.0	106.0 ± 3.0	
	52.094 ± 12	79.806 ± 15	33.539 ± 6	122.1 ± 1.4	111.7 ± 1.4	Fig. 4
	89.286 ± 10	120.031 ± 10	51.058 ± 12	122.7 ± 1.0	115.8 ± 1.0	Fig. 5
			Weighted average:	122.4 ± 0.8		
$F=5$						
	17.786 ± 5	31.979 ± 8	8.096 ± 8	221 ± 8	192 ± 8	
	52.135 ± 12	79.856 ± 15	21.019 ± 4	210.4 ± 1.0	198.6 ± 1.0	Fig. 6
	52.228 ± 8	79.968 ± 10	21.058 ± 5	211.7 ± 1.0	199.9 ± 1.0	Fig. 7
K^{41}	64.272 ± 10	79.962 ± 10				
			Weighted average:	211.1 ± 0.8		

$\Delta\nu_6 = (3386 \pm 30)$ Mc/s; $\Delta\nu_5 = (2396 \pm 15)$ Mc/s
$a = -(502.4 \pm 3.0)$ Mc/s; $b = -(558 \pm 25)$ Mc/s
$\mu_I = +(4.59 \pm 0.05)$ n.m.; $Q = -(0.64 \pm 0.05) \cdot 10^{-24}$ cm^2

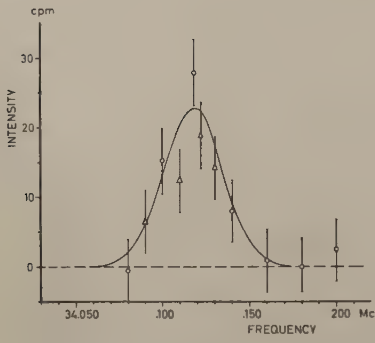

Fig. 8.

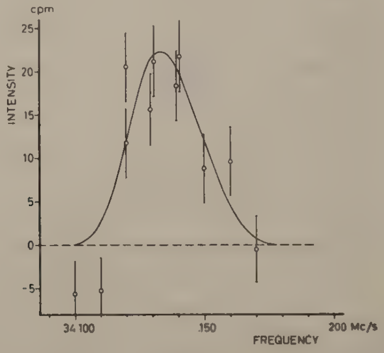

Fig. 9.

Figs. 8, 9. Resonance curves of Bi^{204}, $(F = 15/2)$.

The uncertainty in $\nu''/(\mu_B B/h)^2$ is obtained from the uncertainty in the magnetic field and in the resonance frequency, added quadratically. The uncertainty in the g_J-value has not been taken into account here. In the calculation of the average values, the inverse squares of the uncertainties have been taken as weight factors, and the uncertainty in the mean value is calculated in the usual way.

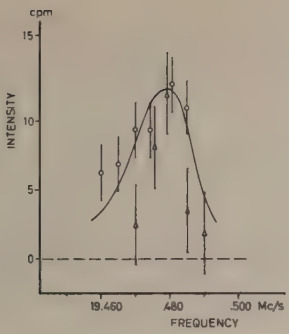

Fig. 10.

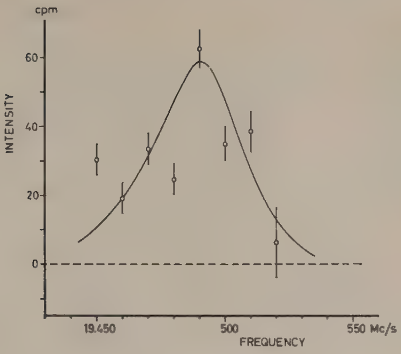

Fig. 11.

Figs. 10, 11. Resonance curves of Bi^{204}, $(F=13/2)$.

Table 2. Bi^{204}.

Ref.	ν_{ref}	$\dfrac{\mu_B B}{h}$	ν	$\nu'' \Big/ \left(\dfrac{\mu_B B}{h}\right)^2 \times 10^6$		Remarks
				$\mu_I > 0$	$\mu_I < 0$	
$F=15/2$						
	16.580 ± 6	30.007 ± 10	9.971 ± 12	130 ± 15	110 ± 15	
	26.793 ± 8	45.969 ± 12	15.370 ± 7	129.2 ± 3.8	115.9 ± 3.8	Fig. 1, ref. [1]
	69.611 ± 6	99.836 ± 7	34.118 ± 10	131.1 ± 1.1	124.9 ± 1.1	Fig. 8
	69.682 ± 10	99.912 ± 11	34.133 ± 8	129.9 ± 1.0	123.7 ± 1.0	Fig. 9
			Weighted average:	130.4 ± 0.8		
$F=13/2$						
	16.545 ± 6	29.949 ± 10	5.452 ± 10	178 ± 11	155 ± 11	
 K^{41}	36.860 ± 5 43.373 ± 8	60.277 ± 7 60.278 ± 8	11.301 ± 10	174.8 ± 2.8	163.4 ± 2.8	
 K^{41}	36.845 ± 12 43.352 ± 15	60.256 ± 17 60.256 ± 16	11.291 ± 8	173.2 ± 2.4	161.8 ± 2.4	
 K^{41}	69.628 ± 8 88.838 ± 10	99.854 ± 9 99.856 ± 8	19.478 ± 10	175.9 ± 1.1	169.0 ± 1.1	Fig. 10
 K^{41}	69.767 ± 10 89.026 ± 15	100.005 ± 11 99.999 ± 12	19.490 ± 10	173.9 ± 1.1	167.0 ± 1.1	Fig. 11
			Weighted average:	174.7 ± 0.8		

$\Delta \nu_{15/2} = (2841 \pm 25)$ Mc/s; $\Delta \nu_{13/2} = (2216 \pm 15)$ Mc/s
$a = -(349.0 \pm 2.0)$ Mc/s; $b = -(358 \pm 20)$ Mc/s
$\mu_I = +(4.25 \pm 0.05)$ n.m.; $Q = -(0.41 \pm 0.05) \cdot 10^{-24}$ cm^2

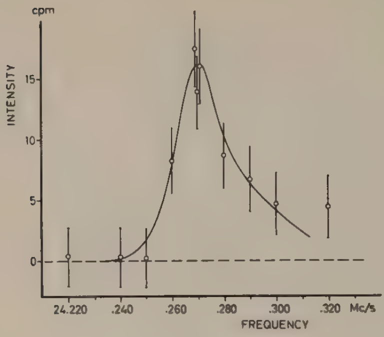

Fig. 12.

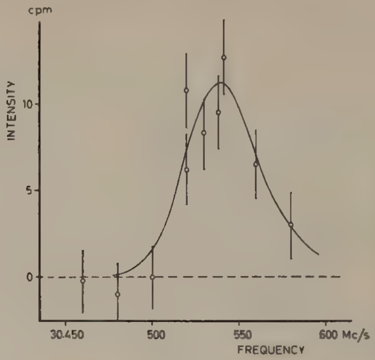

Fig. 13.

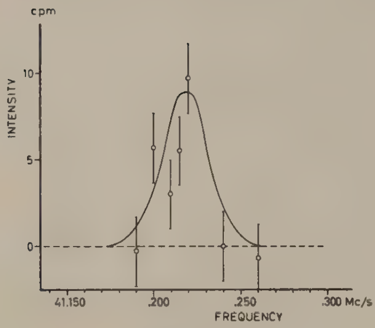

Fig. 14.

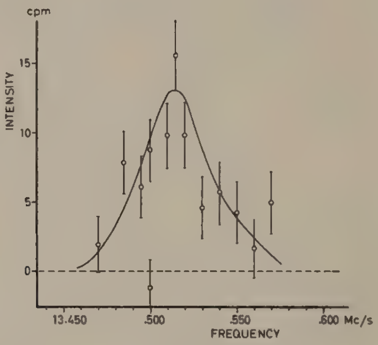

Fig. 15.

Figs. 12, 13, 14. Resonance curves of Bi^{206}, ($F = 15/2$).
Fig. 15. Resonance curve of Bi^{206}, ($F = 13/2$).

The hfs separations and the interaction constants have been calculated by means of equations (1) and (2), and in the calculation of the errors account has also been taken of the uncertainty in the g_J-value. The errors due to the neglect of octupole interaction and of the perturbation of neighbouring states are very small and need not be considered.

The absolute signs of the interaction constants cannot be determined from these measurements, but only the relative signs. According to optical measurements [18], however, the a-value of Bi^{209} is negative, and since the magnetic moment is positive, it follows from equation (3) that the magnetic moment and the a-value have opposite signs for all bismuth isotopes.

The magnetic moments are calculated from equation (3) with the following values of Bi^{209} [8, 17]:

$$I = 9/2,\ a = -446.97 \text{ Mc/s, and } \mu_I = +4.0797 \text{ n.m.}$$

Table 3. Bi^{206}.

ν_{ref}	$\frac{\mu_B B}{h}$	ν	$\nu'' \Big/ \left(\frac{\mu_B B}{h}\right)^2 \times 10^6$		Remarks
			$\mu_I > 0$	$\mu_I < 0$	
$F = 15/2$					
22.834 ± 10	39.972 ± 16	13.328 ± 15	127 ± 10	110 ± 10	
45.725 ± 25	71.915 ± 32	24.270 ± 7	125.2 ± 2.6	116.0 ± 2.6	Fig. 12
60.603 ± 20	89.816 ± 23	30.538 ± 12	127.4 ± 1.9	120.1 ± 1.9	Fig. 13
89.069 ± 12	119.819 ± 12	41.218 ± 12	127.4 ± 1.0	121.8 ± 1.0	Fig. 14
		Weighted average:	127.2 ± 0.9		
$F = 13/2$					
22.836 ± 10	39.975 ± 16	7.308 ± 12	152.5 ± 8.0	134.0 ± 8.0	
45.695 ± 10	71.877 ± 13	13.514 ± 12	153.5 ± 2.5	143.3 ± 2.5	Fig. 15
60.593 ± 10	89.805 ± 12	17.163 ± 12	155.0 ± 1.6	146.8 ± 1.6	Fig. 2, ref. [1]
		Weighted average:	154.6 ± 1.4		

$\Delta\nu_{15/2} = (2914 \pm 25)$ Mc/s; $\Delta\nu_{13/2} = (2411 \pm 20)$ Mc/s
$a = -(374.7 \pm 3.0)$ Mc/s; $b = -(166 \pm 30)$ Mc/s
$\mu_I = +(4.56 \pm 0.05)$ n.m.; $Q = -(0.19 \pm 0.05) \cdot 10^{-24}$ cm^2

The uncertainties given are large enough to include the hfs anomaly, which can be assumed to be small since only p-electrons are involved.

The electric quadrupole moments are calculated from equation (10). The uncertainties are determined with consideration of the uncertainty in the state of intermediate coupling but not of the errors caused by the neglect of Sternheimer's correction or of the effect of configuration interaction.

When not otherwise stated, all quantities in the tables are given in units of Mc/s and the uncertainties in units of the last figure.

The results of Bi^{203} are summarized in table 1, those of Bi^{204} in table 2, and those of Bi^{206} in table 3. The resonance curves at the highest fields are given in figures 4–7 for Bi^{203}, in figures 8–11 for Bi^{204}, and in figures 12–15 for Bi^{206}.

The 14.5 day isotope Bi^{205} is very difficult to produce in quantities large enough for atomic beam experiments. Bi^{206} is always produced at the same time in much larger amounts. In order to obtain enough relative activity of Bi^{205} one must wait several weeks for the shorter-lived Bi^{206} to decay. Only one measurement with Bi^{205} was made with a sample produced by a long irradiation in the cyclotron of the Nobel Institute in Stockholm. This sample was used primarily for spin determinations of Bi^{205} and Bi^{206}. Unfortunately after this measurement this cyclotron was "shut down" for modification, and no further irradiations could be made. Only the $F = 6$ line has been observed at fields high enough to give measurable quadratic effects. The hfs separation $\Delta\nu_6$ can be estimated only very roughly, but it is of the order of 4000 Mc/s, which means that the magnetic moment is about 5.5 n.m.

VI. Discussion

In the nuclear periodic table the bismuth isotopes lie near closed shells for protons as well as neutrons. The nuclei have one proton outside the 82-proton shell and on the neutron-deficient side a small number of neutron holes in the 126-neutron shell. Therefore, the nuclear shell model can be assumed to be a good approximation for these nuclei.

The spin values of the isotopes investigated here are in good agreement with the shell model. The odd-even nuclei of Bi^{203} and Bi^{205} have the spin 9/2 like that of Bi^{209}. This is consistent with the fact that the odd proton is in the level $h_{9/2}$ and that an even number of neutrons have the resultant angular momentum zero. The odd-odd nucleus of Bi^{206} has been investigated theoretically by Wahlborn [21], who obtained the following ground-state configuration,

$$(\pi h_{9/2})(\nu p_{1/2})^{-2}(\nu f_{5/2})^{-1},$$

and the spin value 6, in agreement with the experiments. Bi^{204} is very likely to have an analogous configuration, since the spin value is the same.

It is well-known that the magnetic moment of Bi^{209} is considerably larger than the Schmidt value, in spite of the fact that there is only one particle outside the closed proton and neutron shells. This is probably caused by configurational mixing [22]. Therefore, one cannot expect the extreme single-particle model to give correct values of the magnetic moments of other bismuth isotopes. But with the modified single-particle model, in which the empirical g-values of the odd particles are used, the agreement with experiments is shown to be good. This supports the configuration assignment of the odd-odd isotopes given by Wahlborn. The odd proton moment is taken from Bi^{209}, and the Schmidt value is used for the odd neutron moment, since there is no experimental value of the neutron moment in the $f_{5/2}$ level. Then the values given in the following table are obtained (μ_s is the moment calculated with the Schmidt values and μ_e with the empirical value of the odd proton moment).

Table 4.

Nucleus	Configuration	Experimental moment	Calculated moments	
			μ_s	μ_e
Bi^{203}	$(\pi h_{9/2})(\nu f_{5/2})^{-4}$	+4.59	+2.62	+4.08
Bi^{204}	$(\pi h_{9/2})(\nu f_{5/2})^{-3}$	+4.25	+3.43	+4.77
Bi^{205}	$(\pi h_{9/2})(\nu f_{5/2})^{-2}$	(+5.5)	+2.62	+4.08
Bi^{206}	$(\pi h_{9/2})(\nu f_{5/2})^{-1}$	+4.56	+3.43	+4.77

The single-particle model gives the correct order of magnitude of the electric quadrupole moments only in the vicinity of closed shells. In intermediate regions the deviation can be very large because of collective effects.

For the odd-even bismuth nuclei the single-particle model gives [22]

$$Q \approx -0.25 \cdot 10^{-24}\ \mathrm{cm}^2$$

and for the odd-odd nuclei [22]

$$Q \approx -0.19 \cdot 10^{-24}\ \mathrm{cm}^2.$$

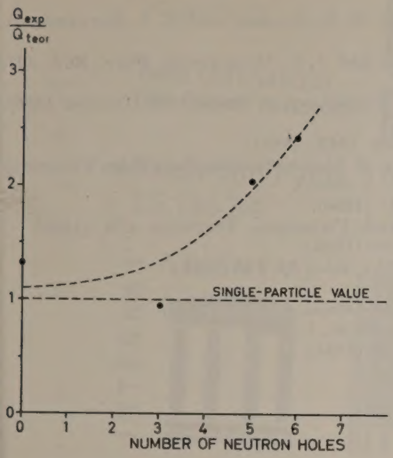

Fig. 16. The ratio of the experimental quadrupole moments to the single-particle values versus the number of neutron holes.

The experimental quadrupole moments are (in units of 10^{-24} cm^2):

odd-even		odd-odd	
Bi^{209}	-0.35 [8]		
		Bi^{206}	-0.19
		Bi^{204}	-0.41
Bi^{203}	-0.64		

In figure 16 the experimental values divided by the single-particle values are plotted against the number of neutron holes. As is to be expected, the quadrupole moments are rapidly increasing with increasing number of neutron holes and are in fair agreement with the single-particle values only very near the closed shells. The deviations can be explained by a small admixture of vibrational states in the ground state of the nuclei.

ACKNOWLEDGEMENTS

The authors are much indebted to Professor Kai Siegbahn for his support and his stimulating interest in this work. Thanks are also due Ingenjör Å. Svanheden and the cyclotron crew of the Gustaf Werner Institute for making numerous irradiations, Dr. K. Smith for valuable private communications, and Fil. kand. S. Axensten for his assistance in taking data.

This work has been financially supported by the Swedish Atomic Committee and U.S. Air Force Research and Development Command.

Institute of Physics, University of Uppsala, Uppsala, Sweden.

REFERENCES

1. C. M. Johansson and I. Lindgren, Nucl. Phys. *9*, 44 (1958/59).
2. A. Lemonick, F. M. Pipkin, and D. R. Hamilton, Rev. Sci. Instr. *26*, 1112 (1955).
3. I. Lindgren, Nucl. Instr. *3*, 1 (1958).
4. J. R. Zacharias, Phys. Rev. *61*, 270 (1942).
5. K. Smith, Report at the Third Molecular Beam Conference at Brookhaven (November 1957).

6. J. P. Hobson, J. C. Hubbs, W. A. Nierenberg, H. B. Silsbee, and R. J. Sunderland, Phys. Rev. *104*, 101 (1956).
7. G. O. Brink, J. C. Hubbs, W. A. Nierenberg, and J. L. Worcester, Phys. Rev. *107*, 189 (1957).
8. K. Smith, Report at the Second Molecular Beam Conference at Brookhaven (October 1956).
9. D. R. Inglis, Phys. Rev. *38*, 862 (1931).
10. D. R. Inglis and M. H. Johnson, Phys. Rev. *38*, 1642 (1931).
11. E. U. Condon and G. H. Shortley, The Theory of Atomic Spectra, Cambridge University Press, London (1935), p. 275.
12. H. Schüler and Th. Schmidt, Z. f. Physik *99*, 717 (1936).
13. H. Kopfermann, Kernmomente, 2. Auflage, Akad. Verlagsges., Frankfurt a.M. (1956).
14. G. Breit and L. A. Wills, Phys. Rev. *44*, 470 (1933).
15. R. Sternheimer, Phys. Rev. *86*, 316 (1952), Phys. Rev. *95*, 736 (1954).
16. G. F. Koster, Phys. Rev. *86*, 148 (1952).
17. N. F. Ramsey, Molecular Beams, Oxford University Press, London (1956).
18. P. Zeeman, E. Back, and S. Goudsmit, Z. f. Physik *66*, 1 (1930).
19. R. G. Barnes and W. V. Smith, Phys. Rev. *93*, 95 (1954).
20. K. Murakawa, Phys. Rev. *110*, 393 (1958).
21. S. Wahlborn, Nucl. Phys. *3*, 644 (1957).
22. R. J. Blin-Stoyle, Rev. Mod. Phys. *28*, 75 (1956).

Tryckt den 27 april 1959

Uppsala 1959. Almqvist & Wiksells Boktryckeri AB